JOURNAL OF MATERIALS SCIENCE 27 (1992) 4305–4310

# Theoretical considerations of thermally stimulated discharge techniques in amorphous semiconductors

C. JUHASZ, B. M. Z. KAMARULZAMAN
*Solid State Research Group, Department of Electrical Engineering, Imperial College of Science, Technology and Medicine, Exhibition Road, London SW7 2BT, UK*

S. M. VAEZI-NEJAD
*Electronic Research Group, School of Engineering, Thames Polytechnic, Wellington Street, London SE18 6PF, UK*

Thermally stimulated discharge of a previously polarized and electroded dielectric, can generate a current with several peaks. The locations of the peaks along the thermally stimulated discharge current spectrum are characteristics of the particular mechanisms for the decay. Systematic analysis of the current peaks will yield information such as dipole relaxation characteristics and activation energies for intrinsic conduction or trapping parameters of electronic charges in the dielectric. When multilayer dielectrics such as amorphous semiconductor photoreceptors are subjected to an electret formation cycle, the heterogeneity in their structures may cause several polarization effects. For example, discontinuities in the intrinsic conductivities and dielectric constant in amorphous selenium (a-Se)-based multilayer photoreceptors can lead to the accumulation of space charges at the interfaces of the individual layers whenever the device experiences an electric stress for a period of time which is of the order of its effective dielectric relaxation time. Charge trapping by states associated with the heterogeneities of the structure cause an electrical polarization which can have a significant impact on the xerographic performance of the photoreceptor. The purpose of the present series of papers is firstly to describe the principles of thermally stimulated discharge techniques, the associated theories and interpretation of the current spectrum and secondly, to discuss applications of these techniques to a-Se:Te/Se double layer photoreceptors. The principles of thermally stimulated discharge and relevant theories are discussed.

## 1. Introduction

There are several experimental techniques for the investigation of the electrical conduction processes in high-resistivity materials and devices. The most common of these are decay methods, time-of-flight methods, contact electrification, direct measurements of $I$–$V$ curves and thermally simulated discharge. Applications of the decay methods and xerographic time-of-flight (XTOF) to amorphous semiconductors have been described previously [1–3].

The purpose of this paper is firstly to demonstrate that thermally simulated discharge (TSD) is a suitable method for investigation of traps, space charge and dipole processes in insulators, and secondly to describe relevant theories on the application of this technique to multilayer amorphous semiconductors.

Experimental results and the method of interpretation are the subject of separate papers.

## 2. Background

### 2.1. Principles of TDS

This technique involves investigation of the charge decay by heating the sample under test at a constant rate. The decay processes are thus investigated as a function of temperature instead of time. The technique can be implemented under open circuit or short circuit conditions as shown in Fig 1. A typical sample in the two configurations is a 10–50 μm film of a few centimetres square area coated on one or both surfaces with evaporated metal alloys. While the classical samples were electrets made of thick plates of carnuba wax or similar substances [4], more recent electret research deals with thick-film polymers such as polyfluoroethylene propylene (PEP), polytetra fluoroethylene (PTFE), polyvinylidene fluoride (PVDF) [5–7] and high-resistivity semiconductors such as amorphous selenium (a-Se) [8, 9]. An electret here is defined as any substance for which the decay time of its stored polarization is long in relation to the characteristic time of experiments performed on the material [10]. Electrets find application in a wide variety of fields such as electret microphones [11], electrophotography [12], gas filters [13], etc.

If $l$ is the sample thickness and $g$ the air gap, then

0022–2461  

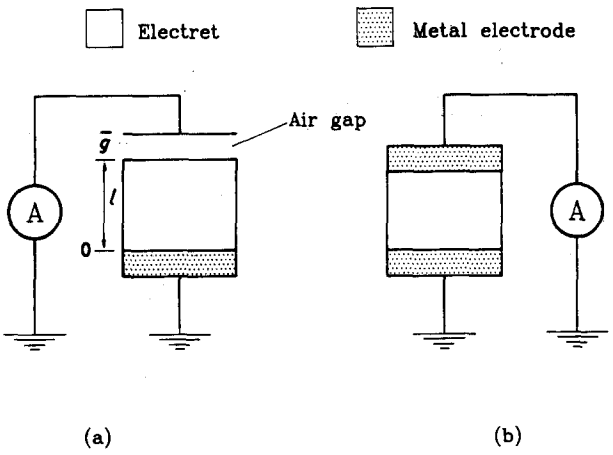


*Figure 1* Physical arrangements for a sample in the TSD experiment.

the integral of the electric field, $E$, for the two configurations in Fig. 1 are given by

$$\int_0^{l+g} E\mathrm{d}x \neq 0, \int_0^{l} E\mathrm{d}x \neq 0, \quad J \neq 0 \qquad (1)$$

for the open circuit electret and

$$\int_0^{l} E\mathrm{d}x = 0, \quad J \neq 0 \qquad (2)$$

for the short-circuit electret. In both cases the measurable experimental quantity is the current density, $J$.

The basic principles of the technique can be best illustrated with the aid of Fig. 2 where the schematic evolution of the following experimental parameters during the polarization and depolarization stages are plotted as a function of time: (a) field across the electroded sample; (b) temperature of the sample; (c) output current across the electrodes. In the polarization stage, the sample, after being electroded, is first heated to some elevated temperature, $T_p$, where it is held at a constant value. In polymers, $T_p$ is normally slightly above the glass transition temperature. A d.c. bias field, $E_p$, is then applied across the electrodes up to a time, $t_p$, after which the temperature of the sample is quickly reduced to a low-value $T_d$ (normally below room temperature) and held constant. The static field, $E_p$, which is still being applied during the cooling down period is then switched off after a total elapsed time, $t_s$. The sample is then short-circuited through a sensitive current meter where it will then be depolarized. In the depolarization stage, the temperature is raised from the time $t_d$ at a constant rate, $t$, typically $4^\circ$C min$^{-1}$ up to and beyond the temperature at which the particular relaxation process under study has ceased to dominate. In most cases, the sample under test would be discarded after a single TSD cycle.

There are several processes which contribute to TSD, the driving force being the restoration of charge neutrality. For example, in polymers the total charge of an electret is usually composed of oriented dipoles and space charge, which cause deviation from local charge neutrality. Before the electret is formed the neutral polymer already contains free charges. At high temperatures these carriers are uniformly generated throughout the entire specimen by disassociation of

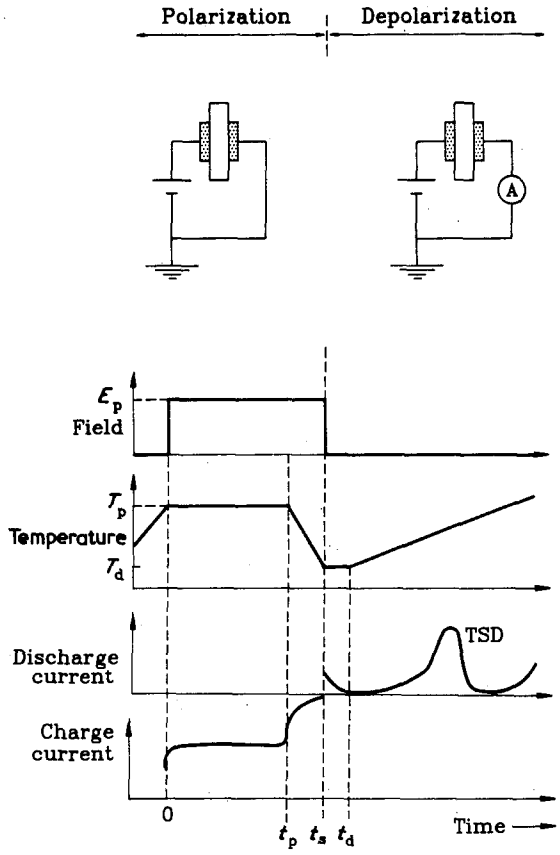


*Figure 2* Principles of the TSD techniques.

neutral entities, resulting in the conductivity of the material, which can be of either an ionic or electronic nature. Therefore, in addition to the excess charges, there must be free equilibrium charges in the electret. These do not contribute to the net charge, but they are responsible for the ohmic conductivity.

The decay of the net charge of an electret during TSD will result from three mechanisms in dipole reorientation, diffusion and drive of excess charge motion and local ohmic conduction. The disorientation of dipoles involves the rotation of a couple pair of positive and negative charges, and requires a certain energy. The space charges are non-uniformly stored, and often reside near the electrodes. During heating they will be mobilized and neutralized either at the electrodes or in the sample by recombination with charges of opposite sign. The forces driving the charges are their drift in the local electric field and diffusion, which tends to remove concentration gradients. The local ohmic conduction neutralizes part of the excess charge by supplying opposed equilibrium charges and does not contribute to the external current during TSD.

## 2.2 Maxwell–Wagner effect

For a heterogeneous system of different layers or phases in the solid dielectric, the decay of the polarization arises from interfacial charges which are accumulated near the interfaces. The unequal conduction currents in the various phases of the system result in the formation of such charges which leads to the so-called interfacial polarization. The physical hetero-

genetics may result from, for example, grain boundaries in polycrystalline solids or fabricated laminates of different amorphous materials, as in the multilayer xerographic photoreceptors.

The phenomenon of interfacial polarization is due to the presence of two phases, one of much higher conductivity than the other. The amorphous phase will give rise to higher mobilities than the crystalline phase. If the amorphous phase contains a sufficiently large number of conducting species, interfacial polarization results, i.e. charge carriers are trapped at phase boundaries. Alternatively, when the material contains many irregularly distributed traps with different depths, as in most polymers, carriers might move in the direction of the field until they fall into deep traps from which they do not have enough energy to escape unless reactivated by a temperature increase. Both these interfacial polarization effects constitute a volume effect. As the Maxwell–Wagner losses are only apparent for low measuring frequencies usually below 1 Hz, the TSD technique is particularly useful in the range of equivalent frequencies of $10^{-1}$–$10^{-4}$ Hz.

### 2.3. Detection efficiency of TSD

The magnitude of the TSD current depends on the effective charge retained by the electret, but not all the decay processes contribute fully to the external current. For example, in decay processes that involve space charges, only part of the decay is observed between the shorted electrets. This experimental characteristic may be due to either one or a combination of the following reasons [13].

(i) Some of the charges could be neutralized by an internal ohmic conduction which will pass unnoticed by the external circuit. This will be especially true for materials of relatively high intrinsic conductivity, like polar polymers.

(ii) Some of the charges may recombine with their image charges at the non-blocking electrodes, therefore only part of the total induced image charge will be free to flow into the external circuit. The nature of the dielectric–electrode interface will thus play an important part in the efficiency of the TSD current measured.

(iii) Current released by diffusion of the excess charges will depend on the blocking nature of the electrodes. A zero external current would result if completely non-blocking electrodes are used.

In general the detection efficiencies for processes involving space charges may be improved by incorporating a highly blocking layer between sample and electrode such that any charge exchange across the electrode–dielectric interface will be blocked. Such a physical arrangement can be easily realized by utilizing an air gap as the blocking layer as shown in Fig. 1a. Also, as the net field in the solid is now non-zero, the decay of excess charges by ohmic conduction can be observed. It has been shown that for such physical systems, decay of the excess charges by internal ohmic conduction will dominate that of drift and diffusion [14]. TSD measurements of this type are often called air-gap TSD or open-circuit TSD.

Alternatively, in such systems, measurement of the voltage induced on the non-contacting electrode would also be useful in the study of the persistent polarization in the sample bulk. This method may be named "charge TSD" because it now measures the evolution of the effective surface charge on the electret as it is being heated up. Compared with the TSD current measurements where the measured signals are very small (typically $10^{-13}$–$10^{-7}$ A), charge TSD has the advantage of measuring large voltage signals (10–$10^3$ V).

## 3. Relevant TSD theories

### 3.1. Theories involving space charge

The TSD decay of a polarization due to excess electrical charges is a more complex phenomenon than that of a decaying dipole polarization. For an understanding of the observed TSD current curves, a satisfactory analytical theory of the movement of excess charges in the dielectric is needed. In addition to the uncertainties in the actual physical processes accompanying the space charge decay, the theory involves solving partial differential equations in the spatial and temporal parameters for the space-charge distribution. No general solution could be derived for the non-linear partial differential equations involved without making simplifying assumptions for the charge-decay mechanisms [14–16].

There are two basic models which are usually considered as starting points for a TSD theory involving space charges. In the charge-motion model, the current is assumed to be essentially governed by the bulk conductivity of the material (electronic or ionic), irrespective of its possible trapping properties. In the trapping model, the current is assumed to result only from carriers (usually electronic) released into the conduction (or valence) band as the charge distribution returns to equilibrium.

#### *3.1.1. The charge-motion model*

The decay of a positive space charge of density $\rho(x, t)$ in a non-polar medium during TSD can be expressed, using the continuity equation as

$$\frac{\partial \rho(x,t)}{\partial t} = -\mu(T)\partial\rho(x,t)E(x,t)/\partial x - \sigma(T)\partial E(x,t)/\partial x \tag{3}$$

where $\mu(T)$ is the drift mobility of the space charges causing the polarization and $\sigma(T)$ is the intrinsic ohmic conductivity of the medium. Both $\mu(T)$ and $\sigma(T)$ are assumed to be thermally activated and obey the Arrhenius shift. The decay of charges via diffusion is neglected in this model. The first term on the right-hand side accounts for the decay of the space charges via a drift (hopping over a single potential barrier) motion while the second term accounts for the decay by ohmic conduction. The electric field, $E$, and the space charge density, $\rho$, are related by the Poisson equation

$$\frac{\partial E(x,t)}{\partial x} = \frac{\rho(x,t)}{\varepsilon_0 \varepsilon} \tag{4}$$

The current density released by the space charge motion is then given by [14]

$$j(t) = \varepsilon_0 \varepsilon \frac{\partial E(x,t)}{\partial t} + [\mu(T)\rho(x,t) + \sigma(T)]E(x,t) \quad (5)$$

Also, because the sample is short circuited

$$\int_0^l E(x,t)\,dx = 0 \quad (6)$$

where $l$ is the thickness of the sample. By integrating with respect to $x$ and using equation 4, Equation 5 can be rewritten as

$$j(t) = [\varepsilon_0 \varepsilon \mu(T)/2l][E^2(l,t) - E^2(0,t)] \quad (7)$$

where $E(0, t)$ and $E(l, t)$ are the values of the electric field at the electrodes obtained by the integration of Equation 4 and using Equation 6. The expression for the current density in Equation 5 also shows that both the displacement and ohmic conduction currents do not contribute to the external current during the TSD.

The partial differential equations describing the actual motion of the space charges can only be solved analytically for very simple charge distributions. The following expression has been obtained for the case of a box distribution of a space-charge cloud whose initial charge density, $\rho(x, 0)$, is constant up to a depth of $f_0$ [14]

$$j(t) = -\mu(T)\rho^2(x_0,t)f(t)^2[1 - f(t)/l]/2\varepsilon_0 \varepsilon l \quad (8)$$

During the decay, the cloud expands into the sample bulk with its leading front, $f(t)$, heading towards the opposite electrode ($x = l$) at a velocity [14]

$$\frac{df(t)}{dt} = \mu(T)E(f,t) \quad (9)$$

$x_0(t)$ is the zero field point, i.e. $E$ at $x_0(t) = 0$, in the sample bulk. From Equation 7 it is also clear that once $f(t)$ reaches the back electrode, at $l$, the current released will abruptly drop to zero. A transit time, $t_\lambda$, is thus defined by the time taken by the leading front, initially at $f_0$ to drift across the sample towards $l$, the back electrode.

For a highly resistive medium ($\sigma(t) \simeq 0$) and $t < t_\lambda$, Equation 5 can also be written as

$$j(t) = \varepsilon_0 \varepsilon \frac{dE}{dt}(l,t) \quad (10)$$

because no charge has reached the back electrode at $l$, $\rho(l, t) = 0$ and the total charge that is released can be found by integrating Equation 10 which yields to

$$Q(t_\lambda) = \varepsilon_0 \varepsilon[E(l,t_\lambda) - E(l,0)] \quad (11)$$

In this model, the amount of charge released will depend on the initial depth of penetration of the excess charges, $f_0$, and the total charge recovered will be a small percentage of the initial charge stored. This percentage would be smaller still if $\sigma(T) = 0$ because internal neutralization caused by ohmic conduction has to be accounted for.

Distributions other than that of the box model have also been considered. For a floating space-charge layer, i.e. one that is touching neither electrode, it has been shown that for the case $\sigma(T) = 0$, the TSD current during $0 \leqslant t \leqslant t_\lambda$ can be expressed as [17–20]

$$j(t) = [\mu(T)\hat{Q}_0/l][E(l,0) - \hat{Q}_0/2\varepsilon_0\varepsilon] \exp\left[(\hat{Q}_0/\varepsilon_0\varepsilon l)\int_0^t \mu(T)\,dt\right] \quad (12)$$

where

$$\hat{Q}(t) = \int_0^l \rho(x,t)\,dx = \varepsilon_0\varepsilon[E(l,t) - E(0,t)] \quad (13)$$

is the total space charge stored, and $\hat{Q}(t) = \hat{Q}_0$ for $t < t_\lambda$. Equation 12 has a temperature dependence similar to that of a single dipole relaxation which implies that the initial part of the TSD plot due to the drift of the space charges can be analysed in the same way as that of the Debye peak of a dipole depolarization. In contrast to the latter, however, the current does not have a linear dependence on the initial magnitude of polarization stored. Another characteristic of the TSD current plot due to the drift of excess charges is that the temperature of the TSD current peak will shift towards a lower temperature as the initial density of stored charges is increased. With a higher density of stored charges, the resulting driving field will be stronger, thus accelerating the drift of the charges towards the electrodes. This results in a faster discharge of the sample.

### 3.1.2. Effect of trapping

The above discussions on the main features of the charge-motion model assume that the discharge current is essentially governed by the drift mobility of the excess charges as well as the intrinsic conductivity of the medium. Any possible trapping effects are neglected by this model. The theory of TSD currents based on trapping models has been extensively discussed by several investigators where it was generally assumed that band-theory concepts are applicable [14, 17, 18]. In this model, a TSD current peak would correspond to a group of electronic carriers that had been previously released from a set of trapping levels within the band gap and was now driven by the internal field towards the electrodes. Unlike the space-charge motion model, which predicted the appearance of only one TSD current peak, a model based on the trapping model can account for the appearance of several TSD current peaks each originating from an ever energetically deeper set of traps.

During the passage of the thermally released carriers towards the shorted electrodes, some of the carriers may experience a series of trapping/detrapping events or they may recombine. The motion of a carrier with fast retrapping can be thought of as a hopping motion and as such, the TSD current expression will be similar to the charge motion model described in the previous section [14]. However, in the trapping model, carrier recombination replaces intrinsic conduction as one of the internal neutralization processes. This similarity of the TSD current expression

again reiterates the caution needed in interpreting TSD data, failure of which will lead to erroneous conclusions.

The case for slow retrapping has also been investigated and again it is noted that for manageable TSD expressions to be obtained, certain drastic simplifying approximations regarding the trapping kinetics, initial charge distribution and nature of electrodes have to be made [17, 18]. It has also been pointed out that unlike the case of a fast retrapping where the TSD current plots are dependent on the initial depth of the excess charge penetration, the TSD plots for the case of slow retrapping are independent of the initial depth of charge, allowing an experimental distinction to be made [14].

## 3.2. TSD of heterogeneous systems

This section considers the TSD behaviour of two types of heterogeneous systems. In the first type, the sample itself is a laminate of two different materials sandwiched between intimately contacting electrodes, while in the second case, the homogeneous solid sample is electroded on only one of its surfaces. If an electrode is brought close and parallel to the free surface, then this physical arrangement can be considered similar to the first class, but now with an air gap as one component of the laminate.

### *3.2.1. Double-layer laminate*

When a heterogeneous structure is subjected to a forming process as that described in Section 2.1, a space-charge layer will be formed at the boundary of the layers. This is usually called a Maxwell–Wagner polarization and is caused by the unequal magnitudes of the ohmic conduction currents entering and leaving the interface, resulting in a net accumulation of charge which may be frozen-in, upon cooling of the sample. Upon removal of the applied field and heating, the accumulated charges can be neutralized by ohmic conduction currents flowing in opposite directions in the respective layers. This neutralization of the interfacial charges will give rise to a peak in the TSD current spectrum. The charging and discharging behaviour of the system is briefly described below.

*3.2.1.1. Charging.* Both layers are assumed to be non-polar and have temperature-dependent conductivities, $\sigma(T)$ and $\sigma_1(T)$, and dielectric constants, $\varepsilon$ and $\varepsilon_1$ (assumed to be temperature independent), respectively. If an applied voltage, $V_a$, is applied across the electrodes, the equilibrium current density within the two layers can be expressed as

$$j(t) = \varepsilon_0\varepsilon_1\frac{dE_1(t)}{dt} + \sigma_1(T)E_1(t) \quad (14)$$

$$= \varepsilon_0\varepsilon\frac{dE(t)}{dt} + \sigma(T)E(t)$$

where $E_1(t)$ and $E(t)$ are the time-dependent electric fields in the layers. These can be related to the applied voltage, $V_a$, by

$$V_a = E_1(t)l_1 + E(t)l \quad (15)$$

where $l_1$ and $l$ are the thickness of the layers.

At the interface, there will be a gradual build-up of a space charge, $Q(t)$, which is assumed to be confined to a thin layer. This means that $E_1(t)$ and $E(t)$ are uniform quantities within their layers and also $Q(t)$ is essentially a surface charge. The build-up of this charge can be described by using the continuity equation which yields to

$$\frac{dQ(t)}{dt} = \sigma_1(T)E_1(t) - \sigma(T)E(t) \quad (16)$$

Also, for the interface, a Gauss law results

$$Q(t) = \varepsilon_0\varepsilon E(t) - \varepsilon_0\varepsilon_1 E_1(t) \quad (17)$$

From Equations 14 and 15, the potential difference across layer 1 can be written as a differential equation

$$\frac{dV_1(t)}{dt} + \beta_g(T)V_1(t) = \beta(T)V_1(0) \quad (18)$$

where

$$\beta(T) = \frac{\sigma(T)}{\varepsilon_0\varepsilon} \quad (19)$$

$$\beta_g(T) = \left[\frac{\sigma_1(T)}{l_1} + \frac{\sigma(T)}{l}\right] \Big/ \varepsilon_0\left(\frac{\varepsilon_1}{l_1} + \frac{\varepsilon}{l}\right) \quad (20)$$

Not that $V_1(0)$ is the capacitively divided value of the applied voltage, at $t = 0$. Using Equation 14 this can also be written as

$$V_1(0) = V_a[1 + (\varepsilon_1/l)/\varepsilon l_1]^{-1} \quad (21)$$

The solution for Equation 15 can be shown to be

$$V_1(t) = [V_1(0) - V_1(\infty)] \exp\left[-\int_0^t \beta_g(T)\,dt\right] + V_1(\infty) \quad (22)$$

Using Equations 15 and 16 and the fact that as $t \to \infty$, $dQ/dt \to 0$ the final equilibrium value of $V_1(t)$ can be expressed as

$$V_1(\infty) = V_a\left\{1 + \left[\frac{\sigma_1(T)}{l} \Big/ \frac{\sigma(T)}{l_1}\right]\right\}^{-1} \quad (23)$$

Using Equations 23, 16 and 17, then as $t \to \infty$, the final charge density established at the interface is given by

$$Q(\infty) = \left\{\frac{1 - [\varepsilon_1\sigma(T)/\varepsilon\sigma_1(T)]}{1 + [l_1\sigma(T)/l\sigma_1(T)]}\right\}\left\{\frac{\varepsilon_0\varepsilon V_a}{l}\right\} \quad (24)$$

Therefore, the magnitude and sign of $Q(\infty)$ will depend not only on the applied voltage, $V_a$, but also on the ratio $\varepsilon_1\sigma(T)/\varepsilon\sigma_1(T)$ being greater or smaller than unity. For a given value of $V_a$, a homocharge or a heterocharge may be obtained at the interface. The sign and magnitude of $Q(\infty)$ will depend on the temperature of the sample via the temperature dependencies of $\sigma_1(T)$ and $\sigma(T)$ (assuming $\varepsilon_1$ and $\varepsilon$ are temperature independent). In the particular case when the individual conductivity curves, $\sigma(T)$ versus $T$,

intersect, the temperature of formation of the electret becomes an important parameter in determining the nature of the interfacial charges than can be stored.

From Equation 24 we also note that $Q(\infty)$ is large when $\sigma(T)$ and $\sigma_1(T)$ differ significantly. For example in an air-gap system where the condition $\sigma_1(T) \gg \sigma(T)$ may be applicable

$$Q(\infty) = \frac{\varepsilon_0 \varepsilon V_a}{l} \tag{25}$$

i.e. the magnitude of the stored charge will be independent of the forming temperature.

*3.2.1.2. Discharging.* During TSD, the frozen-in charges at the interface will be neutralised by thermally generated carriers of the opposite sign which are conveying to the interface by ohmic conduction. Since now the applied voltage is removed

$$V_1(t)l + V(t)l = 0 \tag{26}$$

and also

$$\frac{dV_1(t)}{dt} l_1 + \beta_g(T) V_1(t) = 0 \tag{27}$$

The decay of $V_1(t)$ found from the solution of Equation 27, as a function of temperature $T$ is given by

$$V_1(T) = V_1(t_d) \exp\left[ -\frac{1}{r} \int_{T_d}^{T} \beta_g(T)\, dT \right] \tag{28}$$

$V_1(t_d)$ is the potential difference across layer 1 at the start of the TSD and can be related to the stored interfacial charges by using Equations 15 and 17, yielding

$$V_1(t_d) = \frac{-Q(t_d)}{\varepsilon_0(\varepsilon_1/l_1 + \varepsilon/l)} \tag{29}$$

The current released during TSD is found by substituting Equation 28 into Equation 14

$$j(T) = [\beta_1(T) - \beta_g(T)] \left( \varepsilon_0 \varepsilon_1 \frac{V_1(T)}{l_1} \right) \tag{30}$$

where

$$\beta_1(T) = \frac{\sigma_1(T)}{\varepsilon_0 \varepsilon_1} \tag{31}$$

Substituting for $\beta_1(T)$ and $\beta_g(T)$ into Equation 30 results in the TSD current density

$$j(T) = \left( \frac{\varepsilon\sigma_1(T) - \varepsilon_1\sigma(T)}{\varepsilon_1 l + \varepsilon l_1} \right) V_1(T) \tag{32}$$

From the above Equation it can be seen that the TSD current is the algebraic sum of two opposing currents in the layers. The TSD current is largest, hence the measuring efficiency highest, when $\varepsilon_1\sigma(T)$ differ significantly. The direction of the TSD current will depend on $V_1(T)$ and on the relative magnitudes of $\varepsilon_1\sigma(T)$ and $\varepsilon\sigma_1(T)$. A current reversal in the course of a TSD run will also be possible if the conductivity curves ($\sigma(T)$ against $T$) of the layers intersect as the temperature is increased. This means that the charges are first dominantly neutralized by the ohmic dissipation currents in one layer followed by the dissipation currents in the second layer which is in the opposite direction. When the conductivity curves do not intersect, the TSD current will usually be represented by one asymmetrical peak, the position of its current maximum being determined by the faster of the two ohmic dissipation processes. It can also be shown that the temperature of the current maximum can be expressed as

$$T_m = \left[ \frac{\varepsilon_0 r(\varepsilon_1 l + \varepsilon l_1)[\varepsilon_1\sigma(T_m)A - \varepsilon\sigma_1(T_m)A_1]}{k[\sigma_1(T_m)l + \sigma(T_m)l_1][\varepsilon_1\sigma(T_m) - \varepsilon\sigma_1(T_m)]} \right]^{1/2} \tag{33}$$

where $A$ and $A_1$ are the energies of activation for intrinsic conduction in the respective layers.

The Debye-like character of the decay of the interfacial charges also allows the evaluation of the activation energy for the Maxwell–Wagner relaxation to be approximated by methods that are similar to those used for dipolar disorientation [14].

## 4. Conclusion

Principles and the theories described in this paper serve the basis for the subsequent papers on the application of TSD to multilayer amorphous semiconductors. In this paper, several types of persistent electrical polarization were described.

## References


1. S. M. VAEZI-NEJAD and C. JUHASZ, *J. Mater Sci.* **23** (1988) 3286.
2. *Idem, ibid.* **23** (1988) 3387.
3. *Idem, ibid.* **24** (1989) 471.
4. M. EGUCHI *Phil. Mag.* **49** (1925) 179
5. G. M. SESSLER and J. E. WEST, *J. Electrost.* **1** (1975) 111.
6. G. M. SESSLER (Ed.), "Electicets", Topics in Applied Physics, Vol. 33, (Springer, Berlin, Heidelberg, 1980).
7. R. A. STREET and A. D. YOFFE, *Thin Sol. Films.* **11** (1972) 161.
8. G. GUILLAND, J. FORNAZERO and M. MAITROT, *J. Appl. Phys.* **48** (1977) 3428.
9. Y. HOSHINO and H. MIJATA, *ibid.* **52** (1981) 6214
10. S. MASCARENHAS, in "Electicets", Topics in Applied Physics, Vol. 33, edited by G. M. Sessler (Springer, Berlin, Heidelberg, 1980) Ch. 6.
11. G. M. SESSLER and J. E. WEST, *J. Acoust. Soc. Amer.* **40** (1966) 1433.
12. R. M. SCHAFFERT, "Electrophotography" (Wiley, New York, 1975).
13. J. VAN TURNHOUT in "Electicets, charge storage and transport in dielectrics", edited by M. M. Perlman (Electrochemical Society, Princeton, NJ, 1973) p. 230.
14. *Idem.* "Thermally stimulated Discharge of Polymer Electicets" (Elsevier, Amsterdam, 1975).
15. J. H. CALDERWOOD and B. K. SCAIFE, *Phil. Trans R. Soc.* **269** (1970) 217.
16. B. GROSS, in "Electicets", Topics in Applied Physics, Vol. 33, edited by G. M. Sessler (Springer, Berlin, Heidelberg, New York, 1980 Ch 1.
17. G. F. LEAL FERREIRA and B. GROSS, *J. Non-Metals* **1** (1973) 129
18. G. F. LEAL FERREIRA *ibid.* **2** (1974) 129.
19. R. A. CRESWELL and M. M. PERLMAN, *J. Appl. Phys.* **41** (1970) 2365.
20. G. M. SESSLER and J. E. WEST, *ibid.* **47** (1976) 3480.



*Received 19 April*
*and accepted 5 August 1991*